Supplementary Information

In vivo 2D-IR Spectroscopy of [NiFe] Hydrogenases: A Shielding Role of the Protein Matrix

Mathesh Vaithiyanathan,[a] Cornelius C. M. Bernitzky,[a] Denise Poire,[a,b] Janna Schoknecht,[c] Igor V. Sazanovich,[d] Partha Malakar,[d] Ryan Phelps,[d] Paul M. Donaldson,[d] Gregory M. Greetham,[d] Ingo Zebger,[c] Oliver Lenz,[c] Marius Horch*[a]

[a] Freie Universität Berlin, Department of Physics, Ultrafast Dynamics in Catalysis, Arnimallee 14, 14195 Berlin, Germany. E-mail: marius.horch@fu-berlin.de

[b] Technische Universität Berlin, Department of Chemistry, Modelling of Biomolecular Systems, Straße des 17. Juni 135, 10623 Berlin, Germany

[c] Technische Universität Berlin, Department of Chemistry, Sekr. PC14, Straße des 17. Juni 135, 10623 Berlin, Germany

[d] STFC Central Laser Facility, Research Complex at Harwell, Rutherford Appleton Laboratory, Harwell Campus, Didcot, OX11 0QX, UK

Contents

Experimental Details

Sample Preparation Cells of the SH-overproducing strain *C. necator* HF210 (pGE771) were grown heterotrophically under continuous shaking at 120 rpm in fructose-glycerol-ammonium medium, supplemented with 1µM NiCl, trace element solution SL6, and 1µM ZnCl, as described in [1]. At an OD_{436} of 12, the cells were harvested aerobically by centrifugation and washed twice with 50 mM potassium phosphate buffer, pH 7.0. Finally, the cells were resuspended in the same buffer to a final OD_{436} of ca. 2000 (corresponding to ca. 190 mg/mL of total protein) and frozen in liquid nitrogen.[2]

*Cn*SH was purified from *C. necator* cells as previously described,[1] with the exception that the cell suspension and the crude extract were not kept under an argon atmosphere.

Linear IR Spectroscopy Linear IR absorption spectra were recorded with 2 cm^{-1} spectral resolution using a Bruker Tensor 27 spectrometer, equipped with a liquid nitrogen-cooled mercury-cadmium-telluride (MCT) detector. The sample compartment was purged with dry air, and the sample was held in a temperature-controlled (T = 283 K) gas-tight IR transmission cell for liquid samples (optical path length = 50 µm, volume ≈ 8 µL) equipped with CaF_2 windows. The Bruker OPUS software, version 6.5, was used for data acquisition and evaluation.

2D-IR Spectroscopy 2D-IR spectra were recorded in transmission mode in pump-probe geometry using the ULTRA laser system, as previously described.[3–5] Briefly, two pump pulses with a total energy of 1 µJ were generated by a pulse shaper, and the coherence time τ between them was scanned from 0 to 6 ps with a time steps of 30 fs and an accumulation time of 300 s. The pump beam was spatially overlapped with the probe beam, delayed by a waiting time of T_w = 250 fs, to generate the self-heterodyned 2D-IR signal. *In vitro* 2D-IR spectra of *Cn*SH were recorded using an attenuated probe beam (pulse energy of ca. 100 nJ), while a bright probe beam with a pulse energy comparable to that of the pump pulses was used for recording 2D-IR spectra of *Cn*SH *in vivo*. In addition, a total of eight spectra, obtained as detailed above, were averaged in the latter case. In all experiments, a gas-tight, temperature-controlled (T = 283 K) sandwich cell with CaF_2 windows was used as a sample holder (optical path length = 50 µm, volume ≈ 8 µL). The pump and probe pulses with bandwidths of ca. 300 cm^{-1} and repetition rates of 10 kHz were centred at ca. 2000 cm^{-1}. The pump frequency axis was derived by Fourier transforming the time-domain signal with respect to τ, while the probe frequency axis was obtained by signal dispersion in a spectrograph and detection using two liquid-nitrogen cooled 128-element MCT detectors with a resolution of approximately 2 cm^{-1}. A separate array detector recorded the probe beam for referencing, with the measured laser noise subtracted using the method of Feng et al.[6]

Data Processing To correct for baseline curvature, a cubic spline function was fitted to and subtracted from each pump slice of the two-dimensional dataset. Deriving a diagonal 'cut' spectrum from the 2D-IR data requires interpolation to obtain an n × n data grid and curve fitting to determine the positions and linewidths in the diagonal slices. A cubic interpolation was performed to obtain data points at intervals of 1 cm^{-1} along pump and probe axes, enabling precise extraction of data along the diagonal and anti-diagonal. Gaussian lineshape functions were then fitted to the resulting diagonal and anti-diagonal spectral profiles to determine the associated positions and linewidths. Horizontal pump slices were analyzed to determine transition energies and differences between them for each redox-structural state of the [NiFe] active site. The pump slices were taken at positions determined by the fit to the diagonal slice.

Supplementary Figures

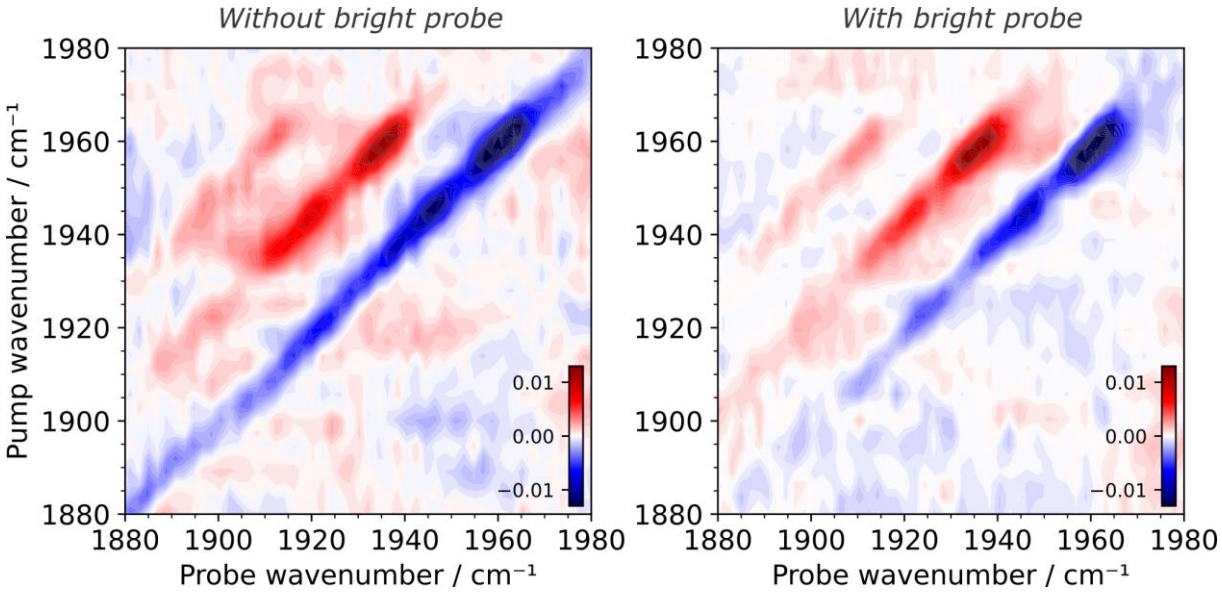

Figure S1: 2D-IR data of *Cn*SH in living cells of *C. necator* recorded without a bright probe beam (left) and with a bright probe beam (right). Note that the data shown in Fig. 2B represent an average of eight datasets, whereas the data presented here are unaveraged. 2D-IR spectra were recorded with parallel pump-probe polarization at T_W = 250 fs.

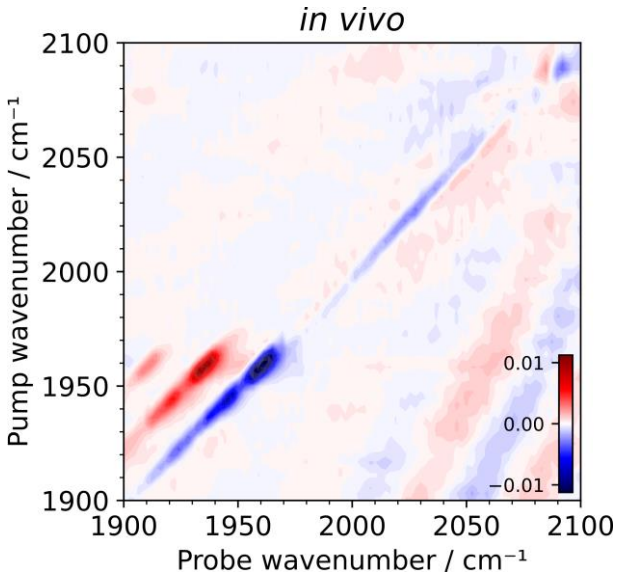

Figure S2: 2D-IR spectrum of *Cn*SH in living cells of *C. necator*. The data are identical to those shown in Figure 2B but extended to the spectral region reflecting CN stretching modes, the most intense of which are seen around 2090 cm^{-1}.

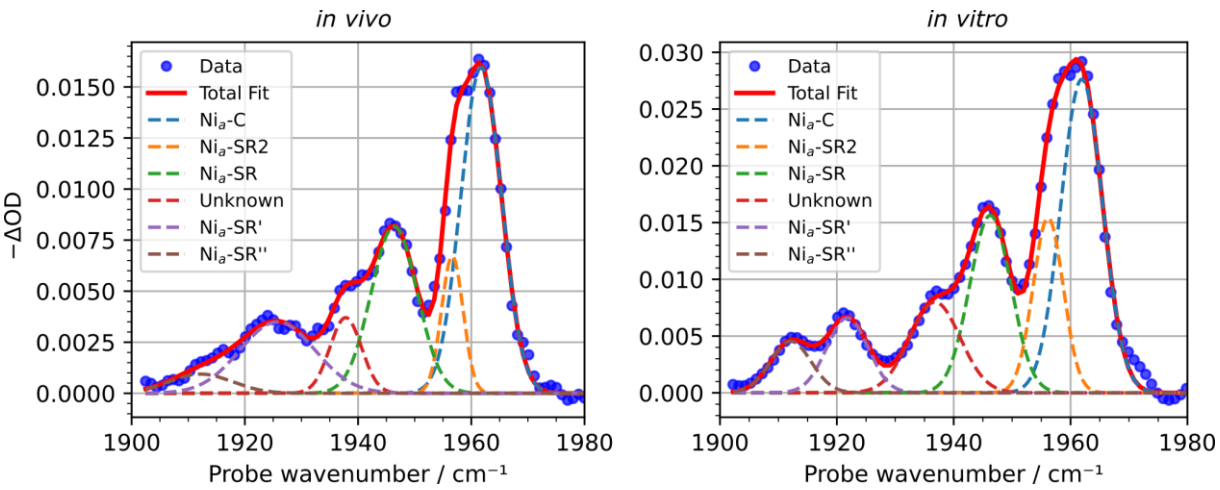

Figure S3: Gaussian fits of diagonal slices from the 2D-IR data shown in Fig. 2B,F. Left: *Cn*SH in living cells of *C. necator*. Right: purified, NADH-reduced *Cn*SH.

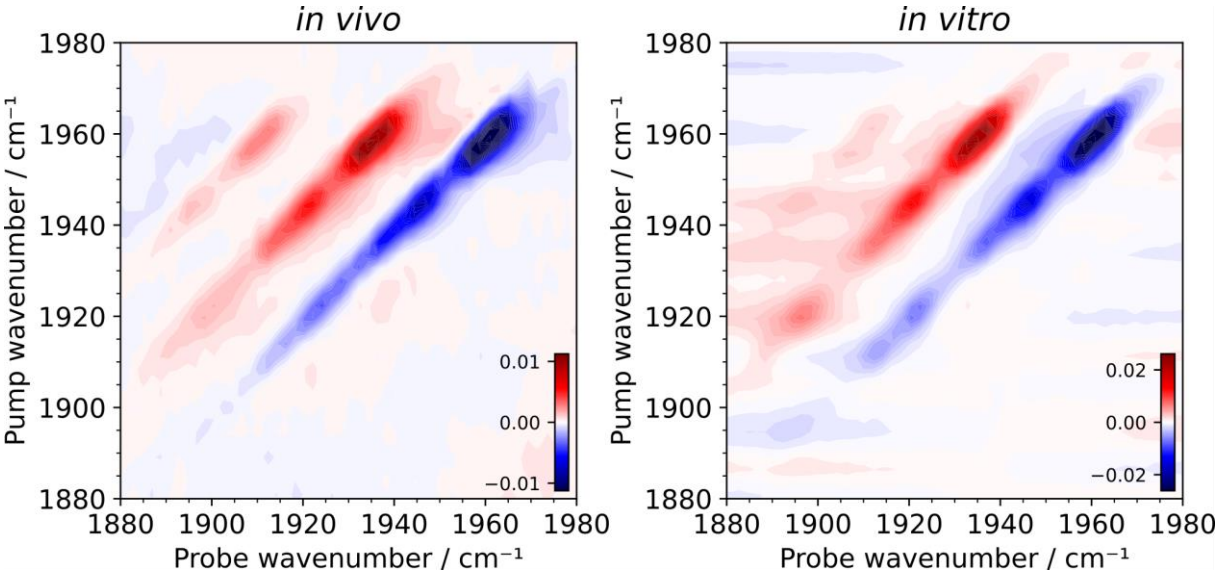

Figure S4: Non-interpolated 2D-IR spectra of *Cn*SH in living cells of *C. necator* (left) and purified, NADH-reduced *Cn*SH (right). The data represent the same experiments as those shown in Fig. 2B,F.

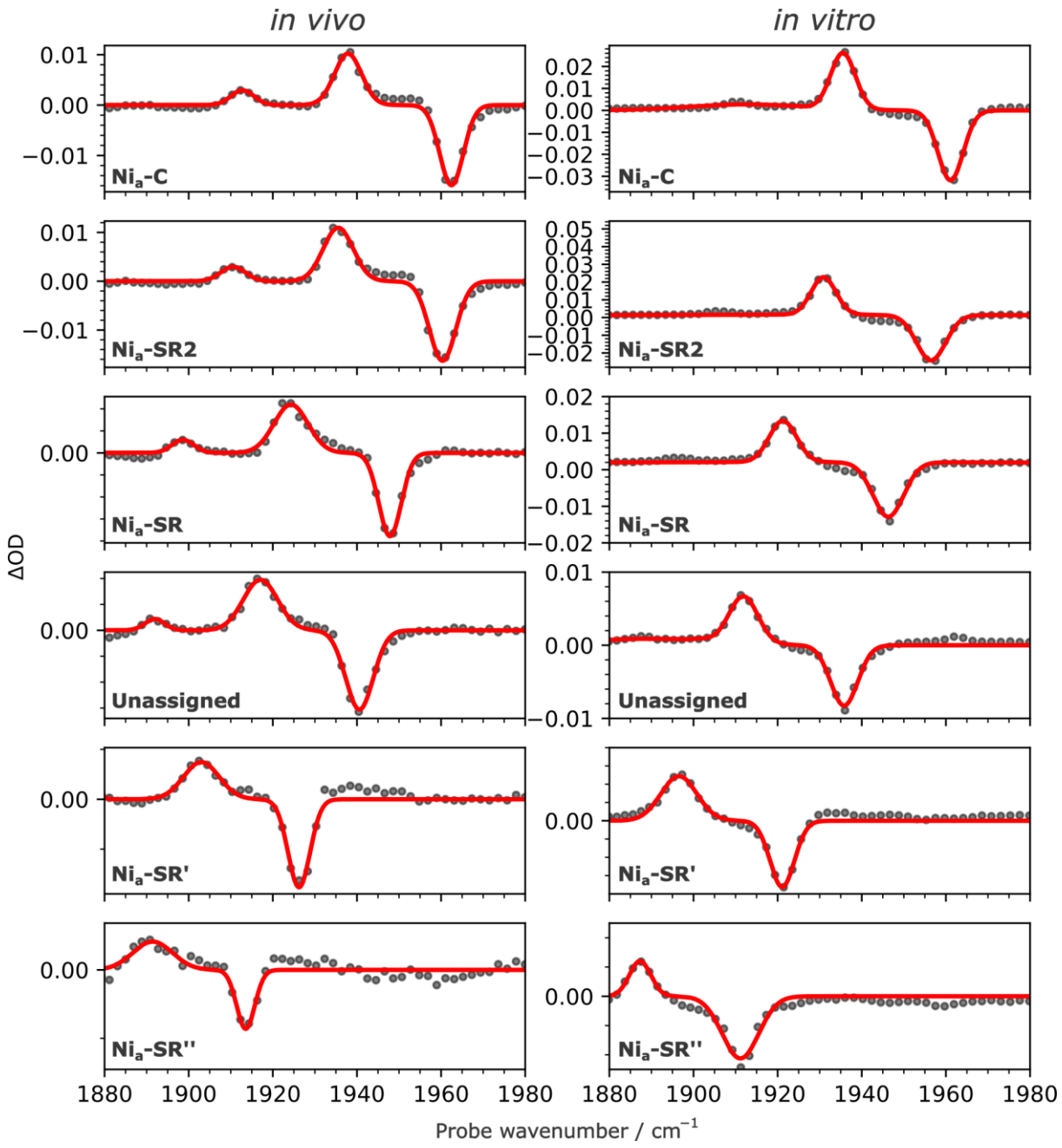

Figure S5: Pump slices from *in vivo* and *in vitro* 2D-IR spectra of *Cn*SH, as shown in Fig. 2B,F. Raw data are depicted as grey dots and fits as red lines. The latter were obtained as linear combinations of Gaussian lineshape functions and used to determine the transition energies listed in Table S1.

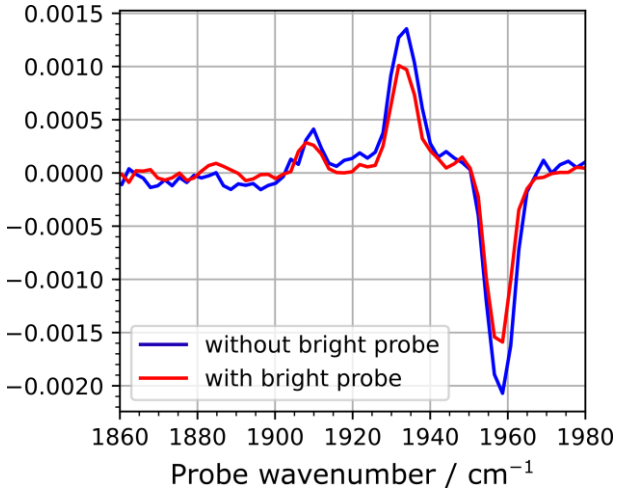

Figure S6: Pump slices (1958 cm^{-1}) from *in vivo* 2DIR spectra recorded with and without a bright probe beam. Note that vibrational ladder climbing is more pronounced with the bright probe beam, which is most obvious from the additional signal appearing around 1884 cm^{-1} (3→4 transition).

Supplementary Tables

Table S1: Transition energies and differences between them (anharmonicities).[‡]

	in vivo					*in vitro*				
State	$E_{0\to1}$	$E_{1\to2}$	$E_{2\to3}$	ΔE_1	ΔE_2	$E_{0\to1}$	$E_{1\to2}$	$E_{2\to3}$	ΔE_1	ΔE_2
Ni_a-C	1962.47±0.12	1937.86±0.21	1912.77±0.65	24.61±0.24	25.09±0.68	1962.09±0.12	1936.49±0.14	1911.97±1.46	25.6±0.18	24.52±1.45
Ni_a-SR2	1960.36±0.14	1935.53±0.22	1910.53±0.72	24.83±0.26	25.00±0.75	1957.48±0.14	1932.07±0.32	1906.93±2.25	25.41±0.35	25.14±2.27
Ni_a-SR	1947.85±0.10	1922.82±0.32	1898.60±0.58	25.03±0.33	24.22±0.66	1947.35±0.13	1922.30±0.23	1897.34±1.80	25.05±0.26	24.96±1.81
n.a.	1940.580.15	1917.05±0.26	1891.90±0.86	23.53±0.30	25.15±0.89	1936.93±0.13	1912.79±0.18	1888.62±1.91	24.14±0.22	24.17±1.91
Ni_a-SR‘	1926.24±0.14	1903.00±0.41	1878.26±1.00	23.24±0.43	24.74±1.08	1922.21±0.10	1897.87±0.17	1874.90±2.09	24.34±0.20	22.97±2.09
Ni_a-SR‘‘	1913.520.26	1889.44±1.25	-	24.08±1.28	-	1912.29±0.19	1888.56±0.26	-	23.73±0.32	-

[‡] $E_{m\to n}$ – transition energies between vibrational energy levels m and n. $\Delta E_1 = E_{0\to1} - E_{1\to2}$. $\Delta E_2 = E_{1\to2} - E_{2\to3}$. Transition energies were obtained by fitting a linear combination of Gaussian lineshape functions to (horizontal) pump slices through the 2D-IR spectra (see Fig. 2D,H; Fig. S5). The positions (pump frequencies) of the slices were determined from the maxima identified in the diagonal slices (see Fig. 2C,G; Fig. S3). Note that fundamental transition energies given in the main text were obtained from a Gaussian fit to the diagonal (Fig. S3). All values are given in units of cm^{-1}.

Table S2: Diagonal and antidiagonal linewidths of $E_{0\to1}$ (full width at half maximum) and the ratios between them. Linewidths are given in units of cm^{-1}.

	in vivo			***in vitro***		
State	Diagonal Linewidth	Anti-diagonal Linewidth	Ratio	Diagonal Linewidth	Anti-diagonal Linewidth	Ratio
Ni_a-C	8.46±0.34	3.83±0.15	2.21±0.12	8.36±0.50	3.41±0.04	2.45±0.15
Ni_a-SR2	4.50±0.43	3.49±0.19	1.29±0.14	6.10±0.65	4.15±0.08	1.47±0.16
Ni_a-SR	9.56±0.70	3.92±0.26	2.44±0.24	8.31±0.76	4.37±0.71	1.90±0.35
n.a.	6.58±1.12	3.24±0.32	2.03±0.40	10.22±1.64	3.56±0.55	2.87±0.63
Ni_a-SR‘	15.59±6.06	3.46±0.31	4.51±1.79	8.28±1.09	4.13±0.32	2.00±0.31
Ni_a-SR‘‘	13.13±8.56	2.65±0.67	4.95±3.46	8.17±1.24	4.07±1.41	2.01±0.76

Supplementary References

[1] L. Lauterbach, O. Lenz, *J. Am. Chem. Soc.* **2013**, *135*, 17897.
[2] M. Horch, L. Lauterbach, M. Saggu, P. Hildebrandt, F. Lendzian, R. Bittl, O. Lenz, I. Zebger, *Angew. Chem. Int. Ed.* **2010**, *49*, 8026.
[3] A. Tokmakoff, L. P. DeFlores, R. A. Nicodemus, *Opt. Lett.* **2007**, *32*, 2966.
[4] S. H. Shim, D. B. Strasfeld, Y. L. Ling, M. T. Zanni, *Proc. Natl. Acad. Sci. U. S. A.* **2007**, *104*, 14197.
[5] P. M. Donaldson, R. F. Howe, A. P. Hawkins, M. Towrie, G. M. Greetham, *J. Chem. Phys* **2023**, *158*, 114201.
[6] Y. Feng, I. Vinogradov, N.-H. Ge, W. S. Chan, T. K. Yee, *Opt. Express,* **2017**, *25*, 26262.